



HAL
open science

Lateral Touch and Frictional Vibrations of Human Fingerprints

François Martinot, Patricia Plénacoste, Christophe Chaillou

► **To cite this version:**

François Martinot, Patricia Plénacoste, Christophe Chaillou. Lateral Touch and Frictional Vibrations of Human Fingerprints. [Research Report] RR-5640, INRIA. 2005, pp.16. inria-00070367

HAL Id: inria-00070367

<https://inria.hal.science/inria-00070367>

Submitted on 19 May 2006

HAL is a multi-disciplinary open access archive for the deposit and dissemination of scientific research documents, whether they are published or not. The documents may come from teaching and research institutions in France or abroad, or from public or private research centers.

L'archive ouverte pluridisciplinaire **HAL**, est destinée au dépôt et à la diffusion de documents scientifiques de niveau recherche, publiés ou non, émanant des établissements d'enseignement et de recherche français ou étrangers, des laboratoires publics ou privés.



INSTITUT NATIONAL DE RECHERCHE EN INFORMATIQUE ET EN AUTOMATIQUE

*Lateral Touch and Frictional Vibrations
of Human Fingerprints*

François MARTINOT

N° 5640

Juillet 2005

Thème Cog

*R*apport
de recherche



Lateral Touch and Frictional Vibrations of Human Fingerprints

François MARTINOT¹, Patricia PLÉNACOSTE², Christophe CHAILLOU³

Thème Cog D – Systèmes cognitifs
Projet ALCOVE

Rapport de recherche n° 5640 – Juillet 2005 - 16 pages

Abstract: In this report, we experimentally show that human fingerprints play a significant role in the lateral touch vibratory mechanisms and that direction of movement results in different dynamic strains on the pulp. Sources that generate sound at the interface are first empirically identified and a spherical model of the index finger is proposed to forecast the radiated fields. Then, haptic sounds are recorded using a miniature microphone placed in the near field. Results are compared with vibrometric measurements carried out in quite similar conditions to assess of the results relevance. Results show that fingerprints can't be neglected in the tribologic interaction. Finally, this research provide a useful information for tactile displays designers and offers future investigations perspectives in many research fields linked with the haptic science.

Keywords: haptics, lateral touch, fingerprint, sound, vibration, tribologic interaction

¹ Author1 affiliation – francois.martinot@lifl.fr

² Author2 affiliation – patricia.plenacoste@lifl.fr

³ Author3 affiliation – christophe.chaillou@lifl.fr

Toucher latéral et vibrations frictionnelles des empreintes humaines

Résumé: Dans ce rapport, nous montrons expérimentalement que l’empreinte humaine joue un rôle important dans les mécanismes vibratoires du toucher latéral et que la direction du mouvement occasionne des déformées dynamiques différentes sur la pulpe. D’abord, les sources de bruit à l’interface de contact sont empiriquement identifiées et un modèle sphérique de l’index est proposé pour prévoir les champs acoustiques émis par le doigt. Ensuite, les sons haptiques sont enregistrés en utilisant un microphone miniature placé en champ proche. Les résultats sont comparés à des mesures vibrométriques effectuées dans des conditions presque similaires pour montrer la pertinence des résultats. Les résultats montrent que les empreintes du doigt ne peuvent être négligées dans l’interaction tribologique. Cette étude fournit finalement des informations utiles pour les concepteurs de périphériques tactiles et offre des perspectives de recherches futures dans de nombreux domaines liés à la connaissance haptique.

Mots clés: haptique, toucher latéral, empreintes, son, vibrations, interaction tribologique.

1 Introduction

One of the main current interests in haptics is to propose an input/output device that could enhance virtual touch interactions by stimulating efficiently the index finger pulp.

Existing proposals [1] have not offered until now any coherence with the real world fingers/textures sliding interactions. Consequently, final users rather experience tickles than real surfaces properties such as roughness. Several mechanical models of the index finger and measurement techniques of its stresses and strains under normal indentation or load have been reported in the literature. However, no result has appeared as regards the dynamic frictions between the skin and surfaces in lateral touch conditions [2].

After a short presentation of current biomechanical finger models and stress/strain sensing techniques, a new sound generation model noise studies is proposed. Then, a microphone is used to identify the vibratory mechanisms involved in the finger/texture tribologic interaction. Signals are compared with vibrometric measurements carried out in quite similar conditions to assess of the microphonic sensing technique relevance for the current and future studies. To finish, results allow to focus on the human fingerprint role and on differences occurring in changes of relative motion directions.

2 Background

2.1 Finger models

The human finger tip is comprised of bone, nail, skin, blood vessels, fat, nerves and sweat glands. The skin of the human finger has a layered structure with the dermis and the epidermis. Dead skin and a series of ridges that made the human fingerprint are located on the surface of the epidermis.

The finger has a viscoelastic memory that results in non linear relationships or hysteresis in stress relaxation and creep. Viscoelastic models of fingers for strains with small amplitude around an equilibrium state [3][4][5] are the most accurate. Among them, the Kelvin model is the most general and consists of a series connection of a dashpot and a spring in parallel with another spring. While these approaches are accurate, numerous local mechanical parameters have to be identified before to run the modelling. Elastic analyses are therefore carried out to get simple models of the human finger. Philips and Johnson modelled the finger as an infinite and homogeneous medium. Srinivasan has proposed a ‘waterbed’ model of the fingertip consisting of a thin membrane enclosing incompressible fluids. Four models of primate fingertip were then developed using finite element methods [6][7]. A quite similar approach was used by Serina [8] and al.. Maeno and al. [9] developed a two-dimensional inhomogeneous finite element model of the fingerpad. Pawluk and Howe [4] also studied the dynamic, distributed pressure response of the fingertip when loaded by a flat surface. They developed an Hertzian model based on their observations and measurements.

2.2 Stress and strain Measurement

In order to validate models, and thus attain a better characterization of the finger’s behaviour, some authors have tried to measure the strain of the structure or the stress at its surface. In this subsection, we present both types of current measurements techniques, before describing a new proposal in the third section.

2.2.1 Force sensors

Work to date has mainly focused on single value force sensors and arrays of integral piezoresistive, capacitive and polymer-based [10] sensing elements. New proposals are mainly Micro-Electro-Mechanical Systems (MEMS) that allow to measure the spatial distribution of forces at the contact area between a finger and a surface. The authors remain voluntary concise about

these technique since “in situ” sensors denature the tribologic interactions encountered in lateral touch conditions.

2.2.2 Optical techniques

Videomicroscopy: Roby, Dandekar, and Srinivasan have placed fine markers on the fingerpad to acquire images of the undeformed and deformed skin. Several indentors impose a static or a dynamic normal load to the pulp. Inspired from previous research in identification of criminals studies [11], Levesque and Hayward [12] have used a digital camera that records the sequence of patterns created by a fingertip as it slides over a transparent surface with simple geometrical features such as a single bump or hole. Skin deformation was measured with high temporal (60Hz) and spatial (88 μ m) resolution by tracking the pulp pores on the fingertip. The patterns of compression and expansion resulting from the presence of a bump or hole were barely discernible. Measurements made with a flat surface have shown that significant strains are present on the index finger even in the absence of a shape. It was unclear whether these measurements were representative of the actual deformations of the fingertip (such as stick-slip of the fingertip ridges) or due to measurement errors and noise.

Colorimetry: Mascaro and Asada [13] have developed Fingernail touch sensors that can detect touch forces at the human fingertip as well as changes in finger posture by measuring the colour pattern of the fingernail. Thus they do not interfere with the human's natural sense of touch.

Vibrometry: In [14], a laser vibrometer was fixed under a skin contactor to measure its vibration amplitude. In an other study [15], the mechanical impedance of the human index finger has been computed using direct measurements along the human index finger under sinusoidal force inputs.

2.2.3 Microphone measurements

In a recent study, small microphones were used [16] to sense sounds internal to the hand produced by gentle fingertip gestures. No reference on fingerpulp frictional sounds has been reported in the literature.

3 Sound radiation from finger

In this section, we investigate the possible use of a microphonic measurement technique to detect the main vibratory mechanisms involved in the sliding interaction of lateral touch. First, we wonder what phenomena generate sounds and predict the radiated fields to efficiently design the experimental setup. Then, a microphonic test bench is proposed for the experiments and comes with a vibrometric another one that allow to directly measure strains in quite similar conditions. Comparisons allow to assess that sound really comes from the skin. To finish, the importance of the fingerprint and directed movements in the dynamics of friction is discussed.

3.1 Sound generation model

3.1.1 Tribologic phenomena

At the interface, several mechanisms create energy which is eventually radiated as sounds. They are characteristic of both surfaces and of their relative motion. Traffic noise studies [17] have related that several sub sources are present when a tire is rolling. By analogy with it and using a simple model of real texture, the sources summarized in Figure 1 and described as follows could be involved:

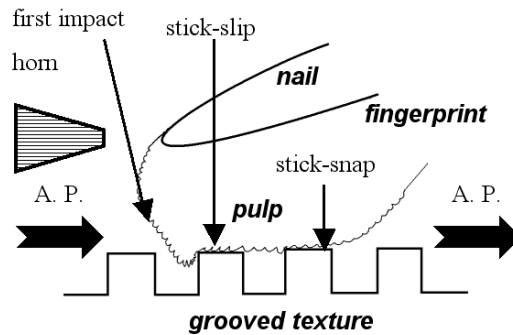


Figure 1. Sound generation model

Fingerprint first impact: while the finger travels on a periodic texture, the bulk finger pulp or fingerprint ridges hit the texture like a viscoelastic hammer.

Stick-slip: within the contact area, the moving finger pulp or finger print ridge transfers tangential forces to the texture while the travelling speed doesn't exceed the local or bulk finger pulp frictional limits.

Stick-snap: adhesion occurs when the skin is sucked in the holes of textures or when other sticking matters are involved in the contact such as sudation of finger or fatty dirtiness deposited on the texture.

Air-pumping (A.P.): air is pumped in and out in the grooves and ridges of both surfaces. When they enter in contact, air is trapped inside the cavities and ejected when the compressed air becomes more rigid than the skin.

3.2 Finger spherical model

Complex noise source are empirically identified. However, it is now necessary to build a simple geometric model to have a representative spatial view of the radiated fields. Results will help to find a good microphone placement for the experiments and will predict possible amplifications or attenuations of the sources contributions to the fields.

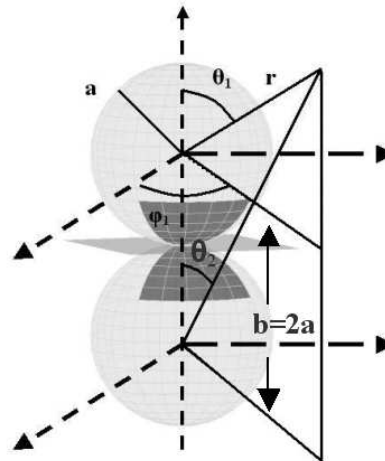


Figure 2. Problem geometry

Spherical models [18] of the tire under dynamic force inputs well describe the radiated field measured in the reality. A similar model seems very well suited for the finger case and we ex-

pect it to predict accurately the radiated fields. System dimensions make indeed difficult to use an acoustic holography measurement technique to check analytical results.

The noise source is defined as a vibration distribution on the contour of the finger modelled as a sphere (Figure 2) with a radius $a=7\text{mm}$. It can be extended or localised. A speed field is imposed on a portion of sphere. It is located at $\theta_0=10^\circ$ of the contact point with an angular extent of 15° in θ_1 and φ_1 . A second sphere allows to take the surface reflection into account.

3.3 Sound field without surface

We first compute the single sphere contribution expressed in terms of spherical modal outgoing wave functions using the following equation (1):

$$p(r, \theta, \varphi) = \sum_{m=0}^{+\infty} \sum_{n=-m}^m A_{mn} h_m^2(kr) P_{|m|}(\cos \theta) e^{jn\varphi}$$

where $h_m^2()$ is the Hankel spherical function of second kind and of order m and $P_{|m|}()$ the Legendre one of order (m,n) .

A radial speed of air particles V_p equal to $V_0=0.1\text{m.s}^{-1}$ is imposed on a surface area close to the contact point ($\theta \in [\theta_0 - \delta\theta_0; \theta_0 + \delta\theta_0]$ et $\varphi \in [\varphi_0 - \delta\varphi_0; \varphi_0 + \delta\varphi_0]$). Using the following formula, we compute the speed amplitudes at the sphere surface.

$$V_p(\theta, \varphi) = -\frac{1}{j\omega\rho} \sum_{m=0}^{+\infty} \sum_{n=-m}^m A_{mn} k h_m^2(ka) P_{|m|}(\cos \theta) e^{jn\varphi} = \sum_{m=0}^{+\infty} \sum_{n=-m}^m V_{mn} h_m^2(kr) P_{|m|}(\cos \theta) e^{jn\varphi}$$

$$V_{mn} = V_0 \frac{(2m+1)(m-|n|)!}{4\pi(m+|n|)!} e^{jn\varphi_0} \frac{\sin(n\delta\varphi_0)}{n/2} \int_{\theta_0-\delta\theta_0}^{\theta_0+\delta\theta_0} P_{|m|}(\cos \theta) \cos \theta \sin \theta d\theta$$

The A_{mn} coefficients values and the first formula allow to determine the pressure spatial distribution :

$$A_{mn} = \frac{j\rho c V_{mn}}{h_m^2(ka)}$$

The sound field radiated is studied in the plane where $\theta_1=90^\circ$ for $r=10$ to 30mm to keep an important sound level. The Figure 3 shows the resulting sound field for different frequencies for a pressure reference equal to $2 \cdot 10^{-5} \text{Pa}$. The radiated field becomes highly directive for higher frequencies than 5kHz .

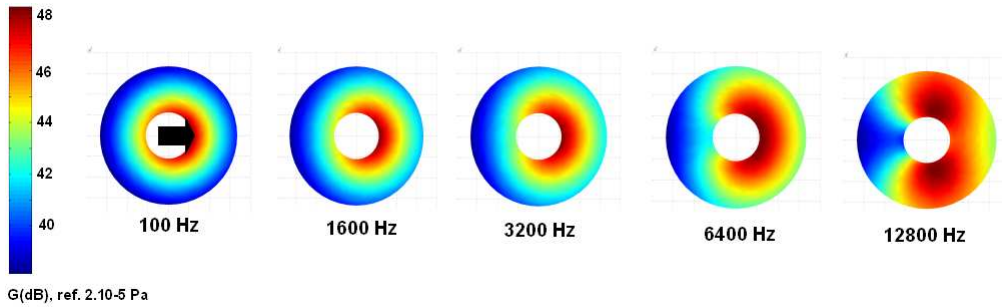


Figure 3. Radiated field without surface for $\theta_1=\pi/2$

3.4 Horn effect with the surface

In this section, we forecast the radiated field using Philippe Klein analytical model [18]. They have been computed using parameters adapted to the sliding finger geometry and possible microphone placements. In this study, the best compromise between the sound level (minimal distance of the microphone) and presence of interferences has to be found. The sound pressure is the sum of contributions from the sphere and its image introduced to fulfil a reflection condition at the road surface.

$$p(r, \theta, \varphi) = \sum_{m=0}^{+\infty} \sum_{n=-m}^m A_{mn} h_m^2(kr) P_{mn}(\cos \theta) e^{jn\varphi} \\ + \sum_{m=0}^{+\infty} \sum_{n=-m}^m B_{mn} h_m^2(kr_2(r, \theta)) P_{mn}(\cos \theta_2(r, \theta)) e^{jn\varphi}$$

Both contributions coefficient are determined by fitting the boundary conditions on the plane surface and on the sphere contour. The radial speed of air particles can be expressed as shown in the following equation:

$$V_p(\theta, \varphi) = -\frac{1}{j\omega\rho} \sum_{m=0}^{+\infty} \sum_{n=-m}^m A_{mn} e^{jn\varphi} \cdot \left\{ \begin{array}{l} kh_m^2(ka) P_{m|n|}(\cos \theta_1) + r \left[\begin{array}{l} k \frac{a-b \cos \theta_1}{r_2(a, \theta_1)} h_m^2(ka) \cdot \\ P_{m|n|}(\cos \theta_2(a, \theta_1)) - \\ b \frac{\sin \theta_1 \sin \theta_2(a, \theta_1)}{r_2(a, \theta_1)^2} h_m^2(ka) \cdot \\ P_{m|n|}'(\cos \theta_2(a, \theta_1)) \end{array} \right] \end{array} \right\}$$

with $B_{mn}=rA_{mn}$ and r the reflection coefficient or porosity factor of the texture. The pressure gain (dB) caused by the presence of texture is shown in Figure 4 ($r=15\text{mm}$) while the pressure reference is the single sphere one. At low frequencies, the sphere does not provide a baffle effect. The sound pressure value is twice the reference one. At higher frequencies the ‘‘piston’’ is baffled by the surface and the sphere. As a result it can cause a peak amplification of 23dB at 12800Hz. So, a microphone placement at $r=15\text{mm}$ and $\varphi_1=90^\circ$ seems to be a relevant choice to carry out analyses in the 10Hz-5kHz frequency range.

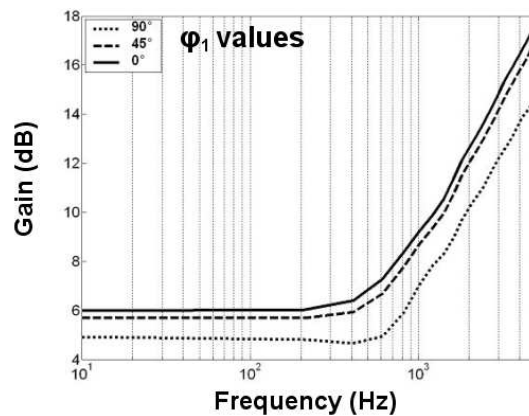


Figure 4. Amplification in the 10Hz-5kHz range

3.5 Experimental setup

Using an experimental approach, we investigate the use of microphonic measurements to understand the tribology of contact in the finger/surface sliding interaction. Results will be compared to vibrometric ones carried out in quite similar conditions.

3.5.1 Apparatus: common features

All the experiments are carried out in a semi-anechoic room. The measured reverberation time is equal to 191ms. In order to analyse the sound field radiated by the finger as a periodic textured surface travels on it and the normal skin stains recorded using a vibrometer, we used a toothed pulley actuated by a Shinsei USR60 ultrasonic motor. The pulley diameter (80mm) is chosen to approximate the contact area as a flat surface. Its surface pattern is a rectangular one (1mm in height) one with a pitch equal to 2.5mm.

Motor choice and speed control: The Shinsei USR60 travelling wave ultrasonic (47kHz) motor does not emit a significant noise in the audible range. Microphonic measurement shows that its frictional sounds frequencies doesn't increase with the motor rotational speed. Above 15rpm, the spectral density of the energy remains constant in all ranges frequencies ($>1\text{kHz}$). Its maximum noise level is equal to $Leq_{100\text{ms}}=52\text{dB(A)}$. As it allows a high torque at low speed (1 N.m at 20 rpm), direct drive is possible [19]. As a consequence, we avoid the additional noise generated by a gear. The pulley rotational speed is measured using an optical encoder directly attached to the rotor. In the following section the speed will be expressed at the pulley periphery ($1\text{rpm}=0.4\text{ cm}\cdot\text{s}^{-1}$).

Force and slope control: A preliminary experiment was carried out to determine a force control method. The toothed pulley alone was laid on a custom-built force sensor and the finger was coated with black ink. The lab jack was lowered from 0.1N by 0.2N to 10N force steps and ink deposits on the index finger were stated on the pulley as shown in Figure 5. When five pulley ridges were in contact, the applied force was between 0.9 and 1.9 N. So, the revolution angle of the jack handle was measured to impose a force comprised in this range on the finger to get comfortable signal levels and avoid wound risks.

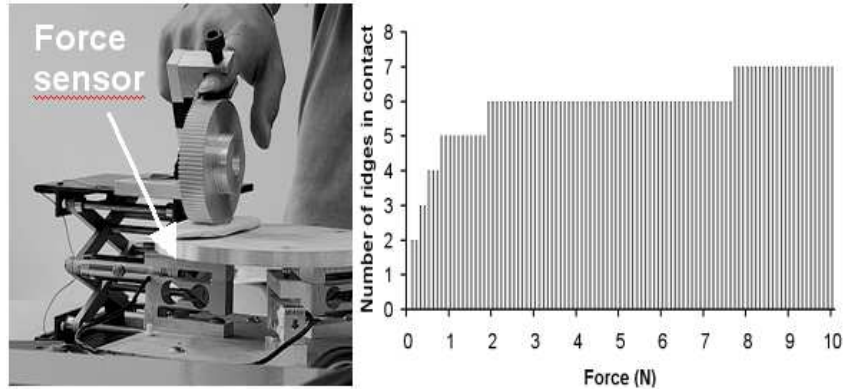


Figure 5. Force control-preliminary study

If it had been easy to control the maximum forces applied to the following experimental device, we have preferred to preserve the system rigidity at the detriment of the force control accuracy.

3.5.2 Microphonic measurement setup

Frictional sounds are recorded using a prepolarised omnidirectional miniature condenser microphone (DPA 4060) with a 5.4 mm vertical diaphragm specially designed for difficult conditions

when mounted directly on the human body (future works). Its equivalent noise level is 23 dB(A) and its sensitivity is $20\mu\text{Pa}$. According to the 3.2.2 subsection, the microphone is placed perpendicularly to the speed field imposed on the finger as shown in Figure 6. The index finger is placed inside the rest notch centred above the pulley.

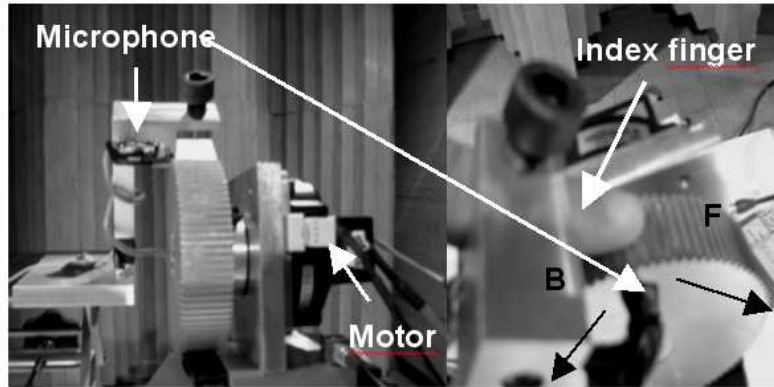


Figure 6. Microphonic measurement test bench

3.5.3 Vibrometric measurement setup

Skin velocity out of the pulp plane is recorded using a single point sensor head (Polytec-PI OFV-505). For the experiment, the skin is coated with black ink to avoid diffraction and reflexions in the skin tissues. It is preferable to record velocities than displacements. Vibrations indeed often generate high displacement amplitudes at low velocities that overload the vibrometer's converters. The sensor head is placed at a 1m distance and the focal point measures approximately $25\mu\text{m}$ on the pulp. The Figure 7 presents the index finger and vibrometer positions.

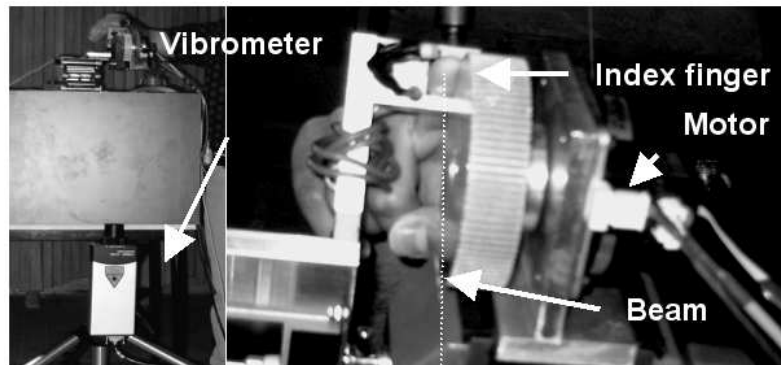


Figure 7. Vibrometric test bench

3.6 Results

Signals have been recorded with the pulley actuated (see figure 6) forward (F) and backward (B) at several speeds (5, 10, 15, 20 and $25\text{cm}\cdot\text{s}^{-1}$). In order to provide a short and representative overview of results, we decide to present results for a F pulley motion at $15\text{cm}\cdot\text{s}^{-1}$. Moreover, microphonic measurements give better result at higher speed ($>15\text{cm}\cdot\text{s}^{-1}$) since signals can be more easily isolated from the low frequency ambient noise.

3.6.1 Fingerprint importance

Depending on fingers and on the location on the pulp, fingerprints ridges are approximately distant from 0.5mm. Both measurement techniques results () clearly show two different periods lengths.

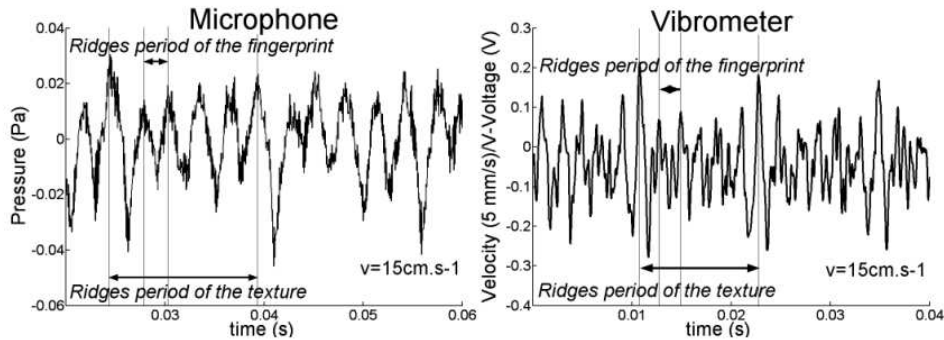


Figure 8. Teeth moving forward, $v=15\text{cm}\cdot\text{s}^{-1}$

A ratio equal to five between texture and fingerprints periods appears at first glance in figure 8. However, the number of pulley teeth in contact has been chosen equal to five too. In order to know the real source of this ratio, we attached the cutting side of a rigid razor edge to a pulley teeth and lowered the lab jack of a 1mm distance to stress the finger with the other side. So, one fine ridge was stimulating the finger pulp. Trials have been carried out at a lower speed ($10\text{cm}\cdot\text{s}^{-1}$) to diminish wound risks. The fingerprint period as been found again in results as shown in Figure 9.

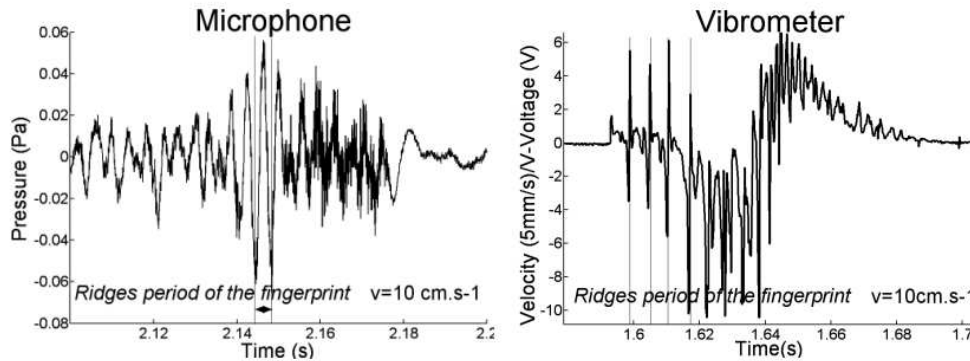


Figure 9. Edge moving forward, $v=10\text{cm}\cdot\text{s}^{-1}$

As explained in the 3.3.4 subsection, if the vibrometric method is able to locally quantify the normal strain of the pulp, displacements measurements for the same experiment remain insensitive to fingerprints ones that are very negligible when compared to the bulk pulp ones as shown presented in Figure 10. This result can explain why haptic researches have always neglected the fingerprints mechanics. However, it is admitted that fast adapting skin mechanoreceptors can sense 75nm strains in lateral touch conditions [20]. As a consequence, fingerprints vibrations may play a significant role in touch perceptions.

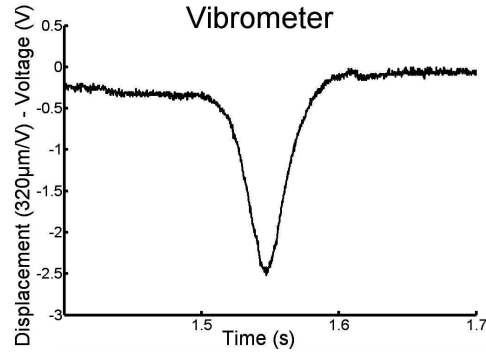


Figure 10. Displacement measurement, $v=10\text{cm.s}^{-1}$

3.6.2 Direction of relative motion

Using the microphonic technique, we have researched if the vibratory phenomena remained similar depending on the motion direction, e.g. forward (F) and backward (B), at $v=15\text{cm.s}^{-1}$. At first glance, temporal signals appeared quite similar. The Fourier analysis revealed that F conditions had quite stationary signals around both surfaces respective periods. B conditions presented very richer spectra. As a consequence, the use of a continuous wavelet transform was investigated to provide a good time – pseudo-frequencies representation. In order to choose the best wavelet for the analysis and to determine the signal class, we first perform a discrete wavelet transform on eight levels and compute the kurtosis values of the details coefficients using the Haar, Meyer, Daubechies 2, 3, 4, Symlets 2, 3, 4 and Coiflets 2, 3, 4. The Meyer's wavelet [21] has been chosen since it is well design for vibratory studies: in this research, it matches signal shapes and has clearly the highest values of kurtosis (>3) in each signal and subband .

The Meyer wavelet presented in Figure 11 is biorthogonal, compactly supported and defined in the frequency domain by:

$$\widehat{\Psi}(\omega) = (2\pi)^{\frac{1}{2}} e^{\frac{i\omega}{2}} \sin\left(\frac{\pi}{2} \nu\left(\frac{3}{2\pi}|\omega| - 1\right)\right)$$

$$\text{if } \frac{2\pi}{3} \leq |\omega| \leq \frac{4\pi}{3}$$

$$\widehat{\Psi}(\omega) = (2\pi)^{\frac{1}{2}} e^{\frac{i\omega}{2}} \cos\left(\frac{\pi}{2} \nu\left(\frac{3}{4\pi}|\omega| - 1\right)\right)$$

$$\text{if } \frac{4\pi}{3} \leq |\omega| \leq \frac{8\pi}{3}$$

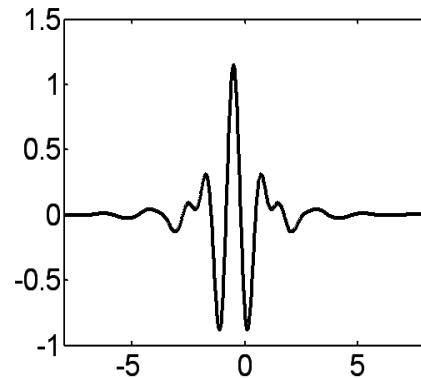


Figure 11. Meyer's wavelet [21]

where $\nu(x) = x^4(35 - 85x + 70x^2 - 20x^3)$, $x \in [0, 1]$

$$\widehat{\Psi}(\omega) = 0 \text{ if } |\omega| \notin \left[\frac{2\pi}{3}, \frac{8\pi}{3} \right].$$

The Figure 12 shows the continuous wavelet transform (CWT) decomposition for F and B conditions. It appears that F conditions involve quite simple elastic vibratory mechanisms around 300Hz while the compressed global structure radiate less energy than moving fingerprints. As expected, the B conditions were very interesting to analyse. Stationary signals are detected in 60Hz and 300Hz. It appears that the impact of the texture ridge is more discernable (60Hz) but that fingerprints radiate less energy. Very coherent events (vertical structures) allow to conclude on transitory chocks occurring at the period of the physical texture.

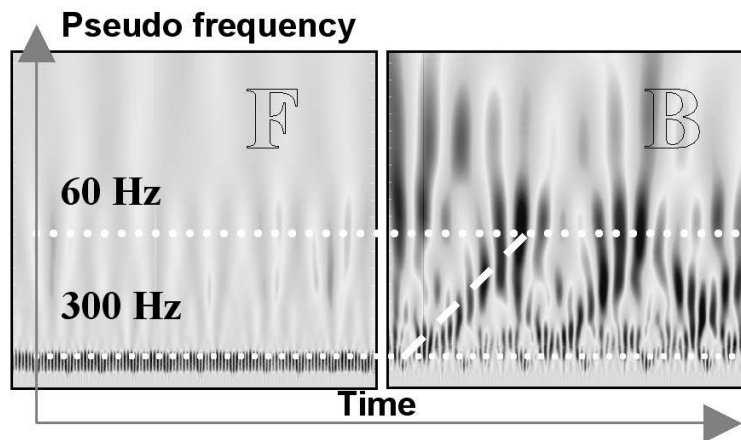


Figure 12. CWT in both directions

The diagonal structures in B are slides toward low frequencies that are compatible with the skin viscoelastic behaviour. Depending on the relative motion direction between the finger and the texture, vibratory mechanisms differs. Touch perceptions may differ too. We believe that touch movements could be closely linked to the fingerprints orientation. Variations in sounds of a thin card edge rubbed on the fingerprint in several directions parallelly or not to its ridges announce a real need of further investigations.

4 Discussion

For the first time in haptics field, we have experimentally studied the vibratory mechanisms involved in a real finger/texture sliding interaction. A new generation model of cutaneous touch sounds has been proposed. An original microphonic sensing technique of dynamic strains on the finger pulp validated by a vibrometric technique and never used until now directly on the finger pulp has been presented. This technique will be use again in more natural interaction contexts.

Surprisingly, the current study has experimentally put forward that human fingerprints play a very important role in mechanical phenomena involved in lateral touch conditions. In 2003, Levesque and Hayward [12] questioned about a possible fingerprint stick-slip on a physical texture. We really believed that their remark was very relevant since our experiments allows to assess that the pulp micro geometry plays a very important mechanical role. Moreover, depending on the movement direction (forward, backward), vibratory mechanisms significantly differs. Human forward movements (B) exhibit viscoelastic mechanical behaviours of the whole structure whereas his backward ones (F) exhibit only quite stationary fingerprints vibrations.

Based on these results, current tactile displays [1] that produce pure sinusoidal forces on the fingerpulp to replicate the lateral touch sliding interaction or use these signals to actuate electromechanical matters that work around a resonant frequency can't provide realistic stimuli to final users. While touching virtual textures, users have indeed to experience fine and complex mechanical forces designed with taking the fingerprints microgeometry and the direction of movement into account. This new finding provide precious information in perceptual and neuropsychological studies. As future works we plan to investigate the influences of finger force, speed, direction and slope of fingerprints on vibratory mechanisms at the interface.

5 Acknowledgements

This work has been carried out within the framework of the INRIA Alcove project and is supported by the IRCICA (Institut de Recherche sur les Composants logiciels et matériels pour l'Information et la Communication Avancée). The authors thank Philippe Klein (PhD-INRETS-LTE-Bron) for his sophisticated knowledge of the horn effect, his useful help and Houzefa Aladine (Undergraduate Student-Centrale Lille) for his technical support in the experiments.

6 References

- [1] Benali Khoudja M., Hafez M., Alexandre J.M., Kheddar A., "Tactile Interfaces. A State of the Art Survey", Proceedings International Symposium on Robotics 2004, Paris, pp 721-726, 2004.
- [2] Lederman S. J., Klatzky R. L., "Hand movements : a Window into Haptic Object Recognition". *Cognitive psychology*, 19, pp 342-368, 1987.
- [3] Moy G., Singh U., Tan E., Fearing R.S., "Human Psychophysics for Teletaction System Design", *The Electronics Journal of Haptics Research* Vol. 1, No. 3, 2000.
- [4] Fung, Y. C., "Biomechanics: Mechanical Properties of Living Tissues", *Springer-Verlag*, pp 41-48, 1993.
- [5] Pawluk, D. T. V., Howe, R. D., "Dynamic Lumped Element Response of the Human Fingerpad" *Journal of Biomechanical Engineering*, 121, pp 178-183, 1999.
- [6] Srinivasan, M. A., "Surface deflection of primate fingertip under line load", *Journal of Biomechanics*, 22, pp 343-349, 1989.
- [7] Srinivasan, M. A., Dandekar, K., "An investigation of the mechanics of tactile sense using two dimensional models of the primate fingertip". *Journal of Biomechanical Engineering*, 118, pp 48-55, 1996.
- [8] Serina, E. R., Mockenstrum, E., Mote, C. D., Rempel, D., "A Structural Model of the Forced Compression of the Fingertip Pulp", *Journal of Biomechanics*, 31, pp 639-646, 1998.
- [9] Maeno, T., Kobayashi, K., "FE Analysis of the Dynamic Characteristics of the Human Finger Pad With Objects With/Without Surface Roughness", *Proceedings ASME Dynamic Systems and Control Division*, DSC-64, pp 279-286, 1998.
- [10] Lee, M.H., Nicholls, H. R., "Tactile sensing for mechatronics – a state of the art survey", *Mechatronics*, 9, pp 1-33, 1999.
- [11] Jain, A., Pankanti S., "Automated fingerprint identification and imaging systems". *Advances in Fingerprint Technology*. Elsevier, New York, second edition, 2001.
- [12] Levesque, J., Hayward, V., "Experimental Evidence of Lateral Skin Strain During Tactile Exploration", *Proceedings Eurohaptics 2003*, pp 261-275, 2003.
- [13] Mascaro, S., Asada, H., 2004. "Measurement of Finger Posture and Three-Axis Fingertip Touch Force Using Fingernail Sensors", *IEEE Transactions on Robotics and Automation*, vol. 20, no. 1, pp 26-35, 2004.

-
- [14] Kyung, K. U., Ahn M., Kwon D.-S., Srinivasan M. A., “Perceptual and Biomechanical Frequency Response of Human Skin: Implication for Design of Tactile Displays”, *Proceedings Worlhaptics 2005*, pp 96-101, 2005.
- [15] Chia-Yu, F., Manny O., “Direct Measurement of Index Finger Mechanical Impedance at Low Force”, *Proceedings Worlhaptics 2005*, pp 657-659, 2005.
- [16] Amento, B., Hill, W., Terveen, L., “The Sound of One Hand: A Wrist-mounted Bio-acoustic Fingertip Gesture Interface”, *Proceedings CHI2002*, pp 724-725, 2002.
- [17] Sandberg, U., J. A. Ejsmond. *Tire/road noise reference book*, Informex, Kisa, Sweden, 2002.
- [18] P. Klein, “Horn effect characterisation for tire–noise radiation”, *Proceedings Internoise*, Nice, 2000.
- [19] Giraud, F., Semail, B., Audren, J.-T, “Analysis and phase control of a piezoelectric traveling-wave ultrasonic motor for haptic stick application”, *IEEE Transactions on Industry Applications*, 40, 6, pp 1541-1549, 2004.
- [20] Biggs S., Srinivasan M. A., “Tangential versus normal displacements of skin: Relative effectiveness for producing tactile sensations”, *Proceedings HAPTICS'02*, IEEE, (2002).
- [21] Meyer Y.. *Wavelets, vibrations and scalings*, CRM Monograph Series, 9, American Mathematical Society, Providence, 1998.